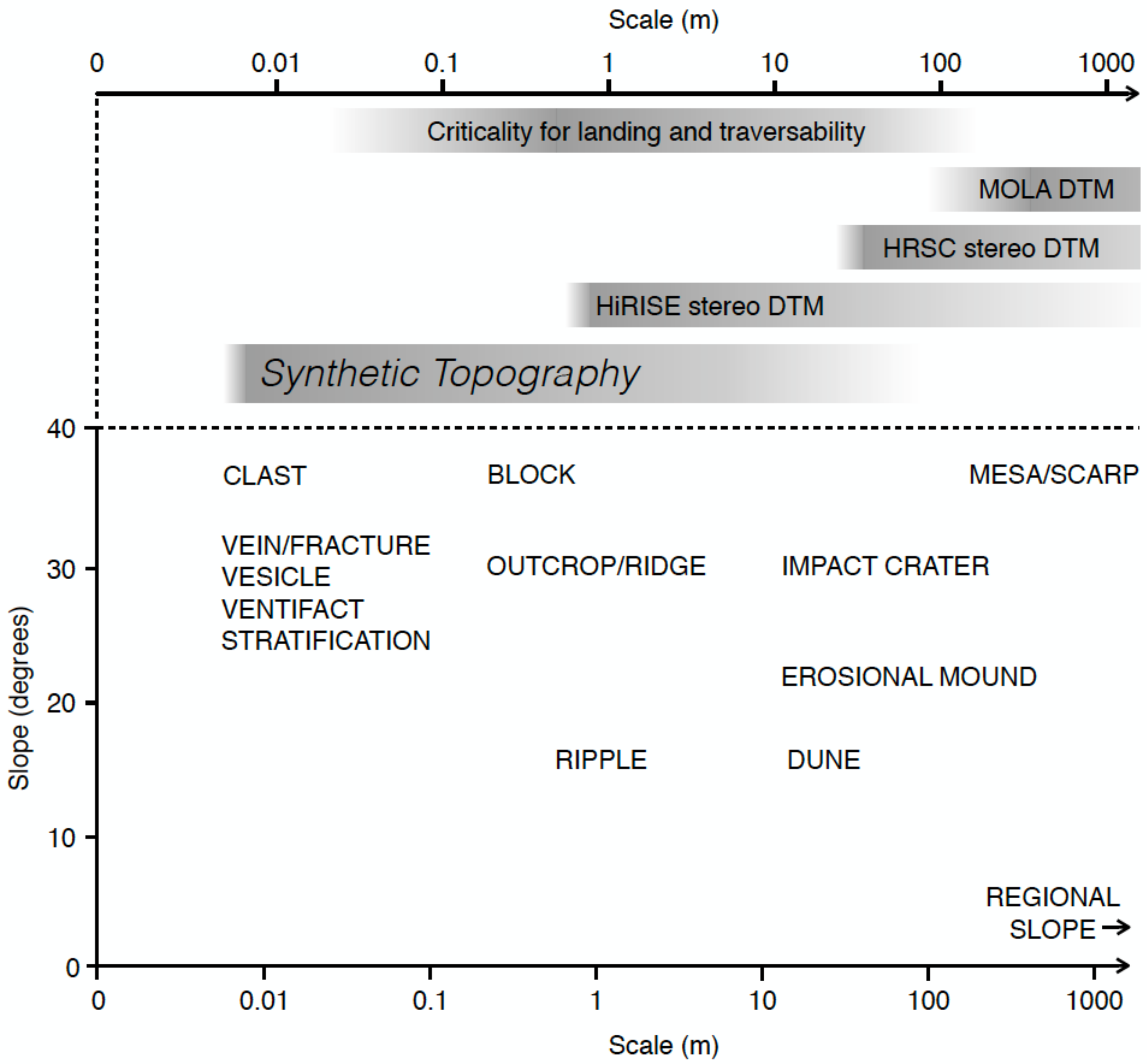

Figure 1. Schematic plot showing the applicability of factors and DTM types at different spatial scales (top), and the approximate placement on slope and size axes of common Mars geologic features (bottom). The need to fill the data gap at ~sub-meter scales, where features are still large enough to be relevant to landing and traversability, is highlighted. This domain is where synthetic topography can play a role.

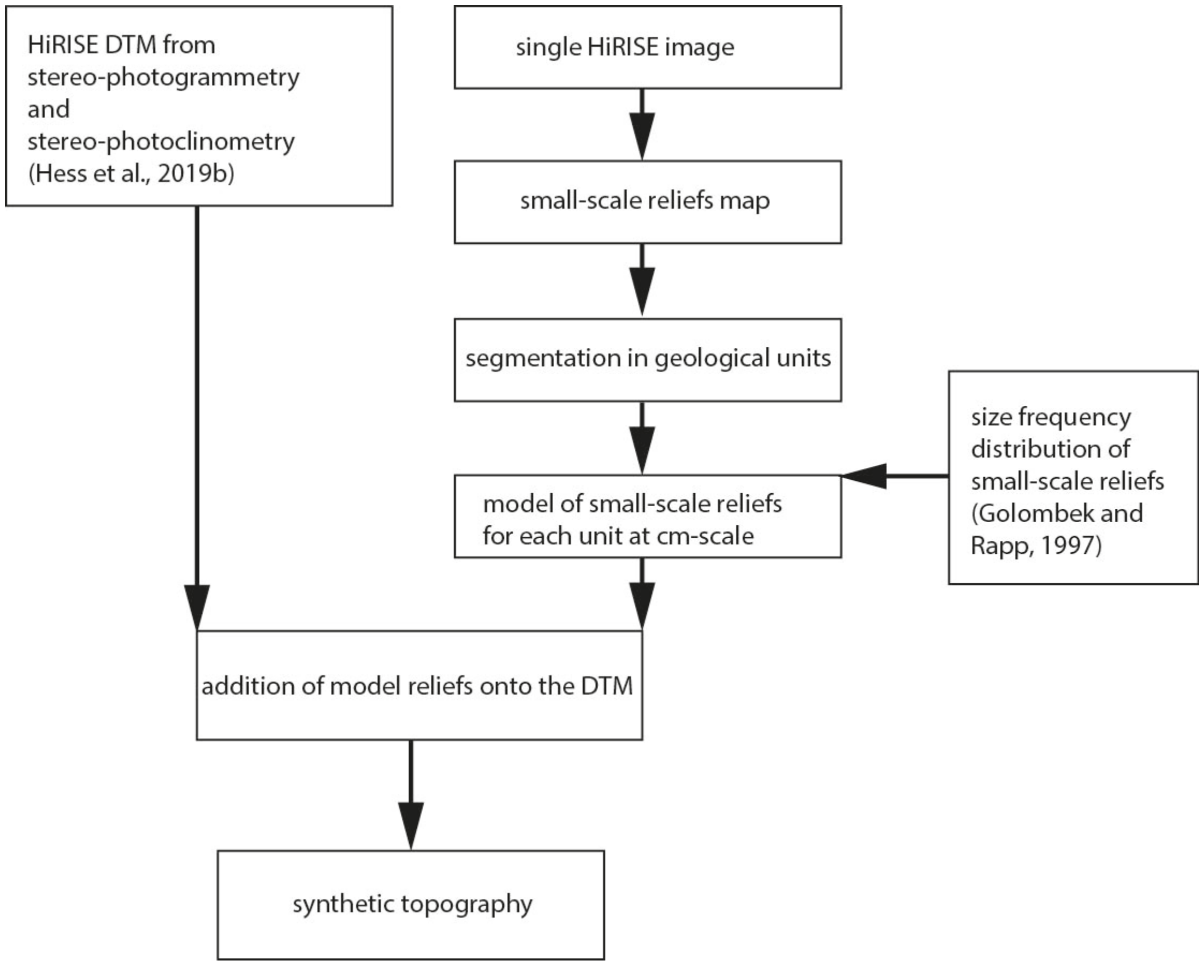

Figure 2. Workflow for the calculation of a synthetic topography using inputs from HiRISE images, a stereo and shape from shading technique, and a model for the abundance of small-scale reliefs.

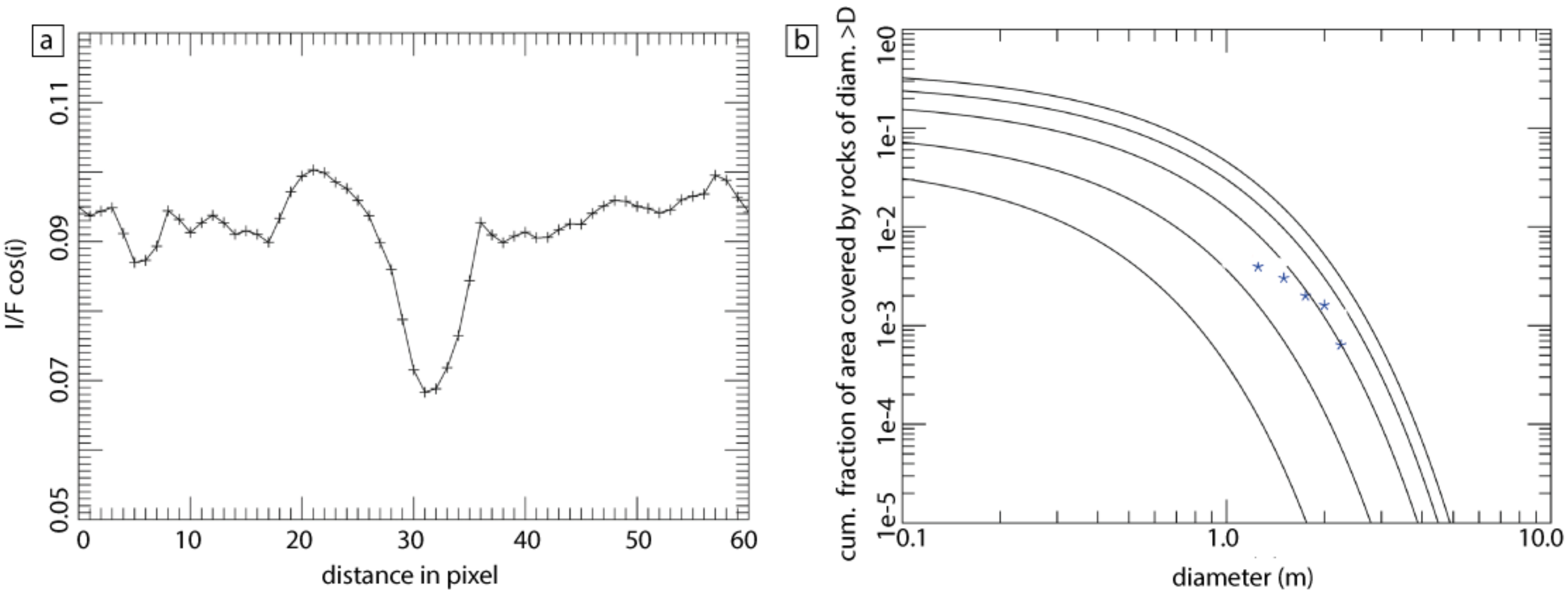

Figure 3. (a) Reflectance profile across a block and its shadow from HiRISE data. Illumination direction from the left. (b) Cumulative fractional area covered by small reliefs larger than a given diameter, as a function of the relief diameter. Curves represent the distribution of reliefs at 5, 10, 20, 30, 40% from Golombek and Rapp (1997). Data points are from a 500 by 500 m^2 area. Downturn at low diameter is a resolution effect.

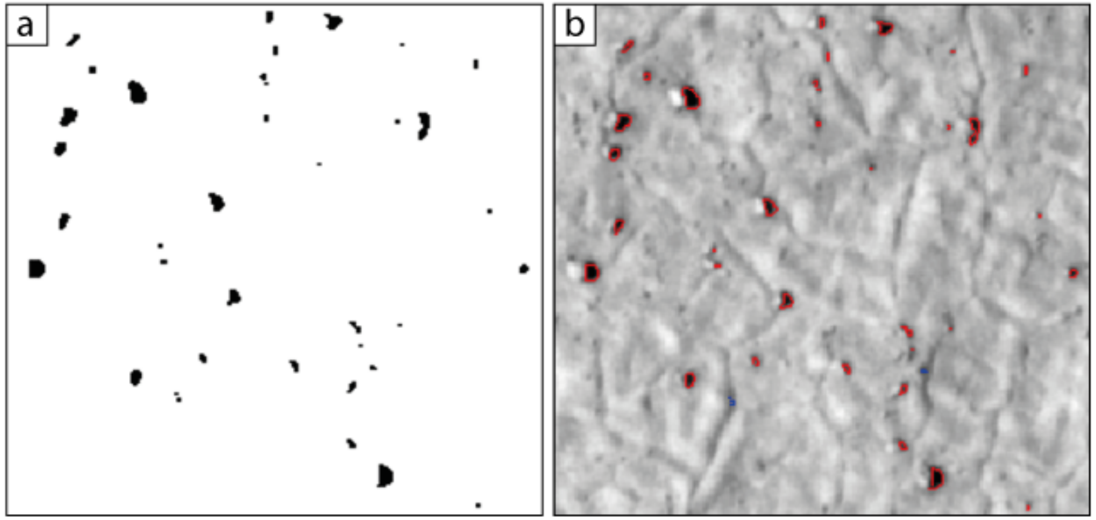

Figure 4. (a) Shadow mask of a 500 by 500 m^2 area. (b) Contours (in red) of identified shadow belonging to blocks overlaid on an HiRISE frame.

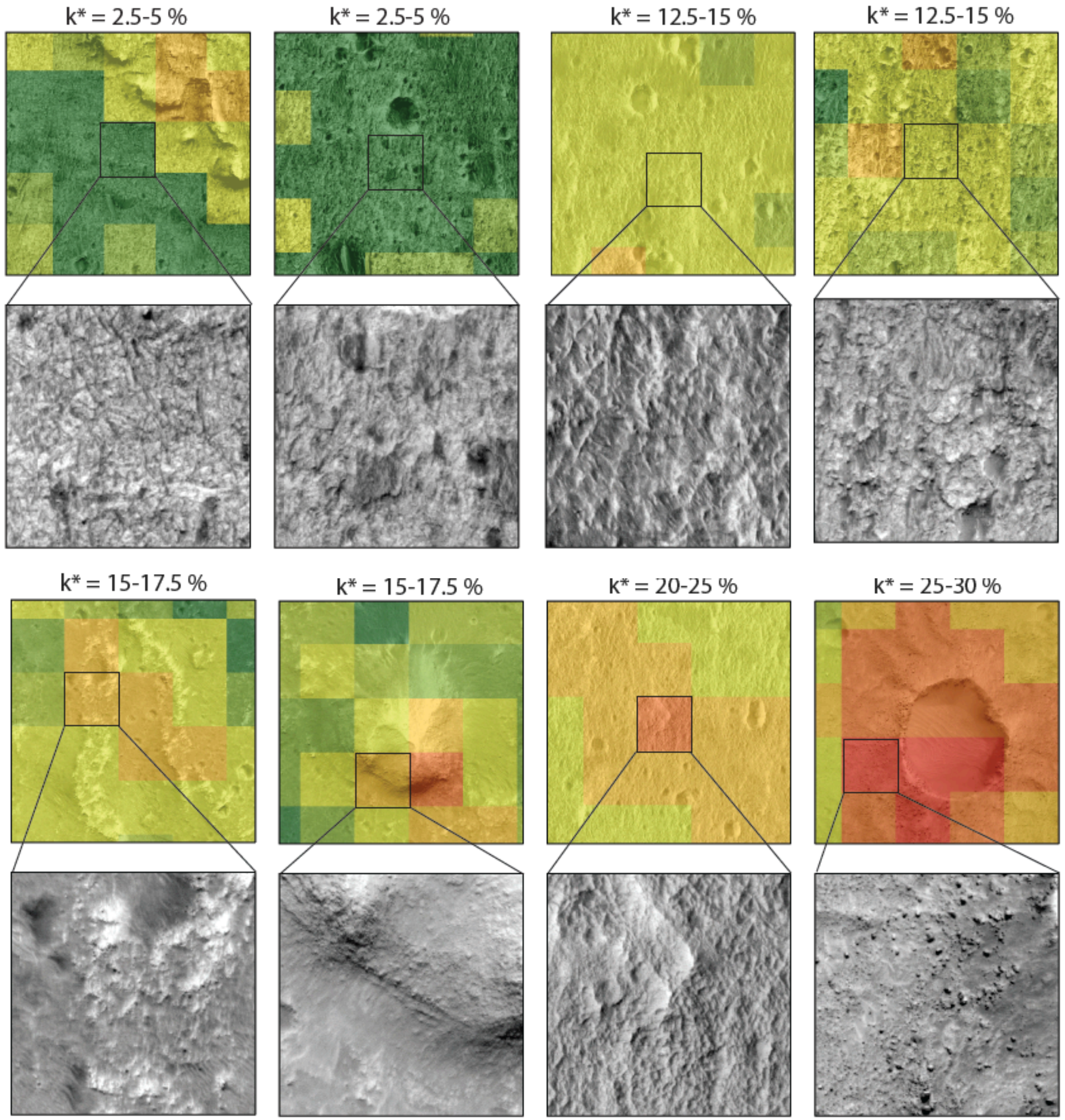

Figure 5. Representative areas for different abundances of shadow-casting reliefs expressed as k* (see text for definition). Abundance maps are color-coded (See figure 6 for labeling). Abundance maps are 500 m wide. HiRISE close-ups are 110 m wide.

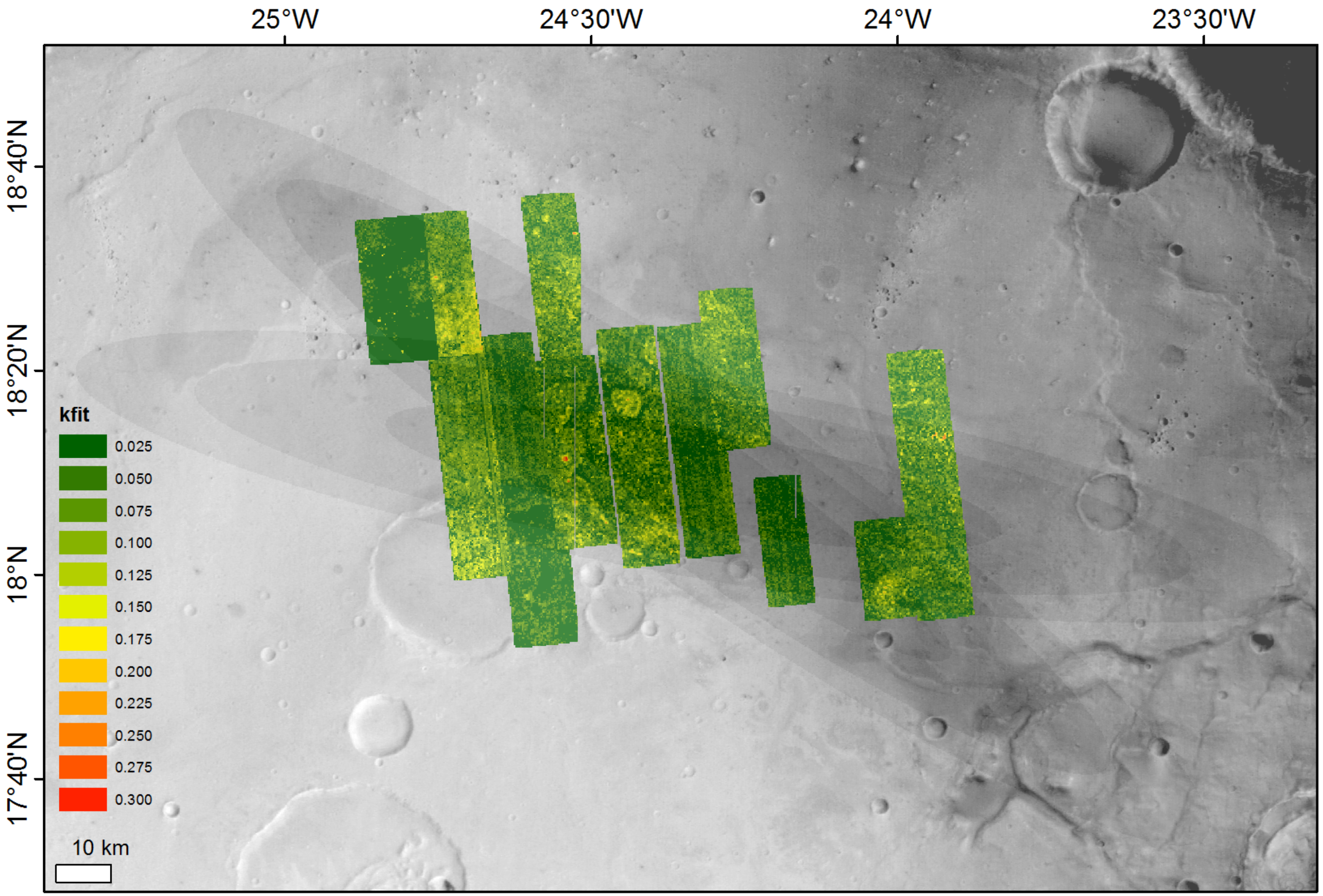

Figure 6. Color-coded maps of cumulative fractional area of reliefs superimposed on a High Resolution Stereo Camera (HRSC) mosaic (Gwinner et al., 2016, 2019). The landing site ellipses for a 2020 launch are shown for different landing probability (light gray: 3-sigma, medium gray: 2-sigma, dark gray: 1-sigma). The azimuth of the ellipses is a function of the launch date.

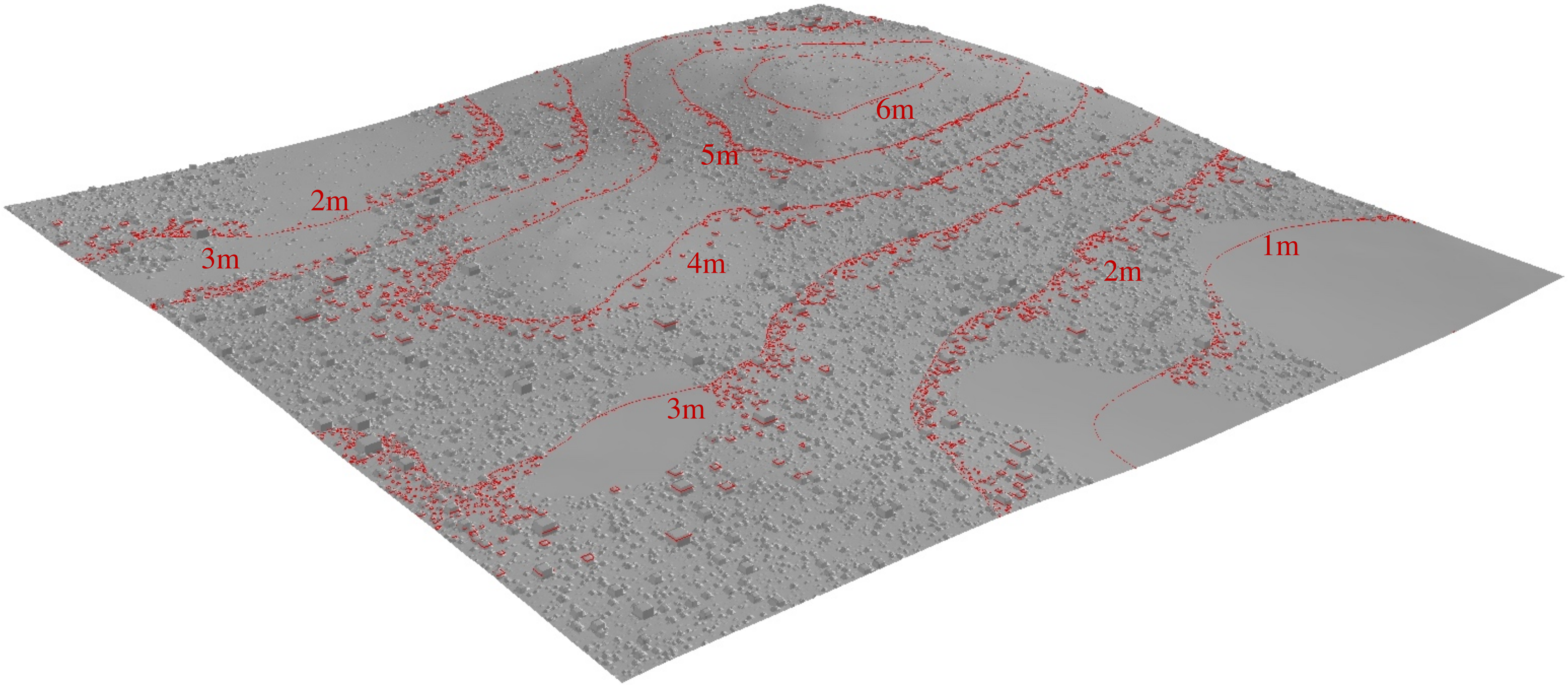

Figure 7. Perspective view of a shaded relief from the synthetic topography at a spatial resolution of 1 cm over an area of 100x100 m^2. Red contour lines are shown every meter.

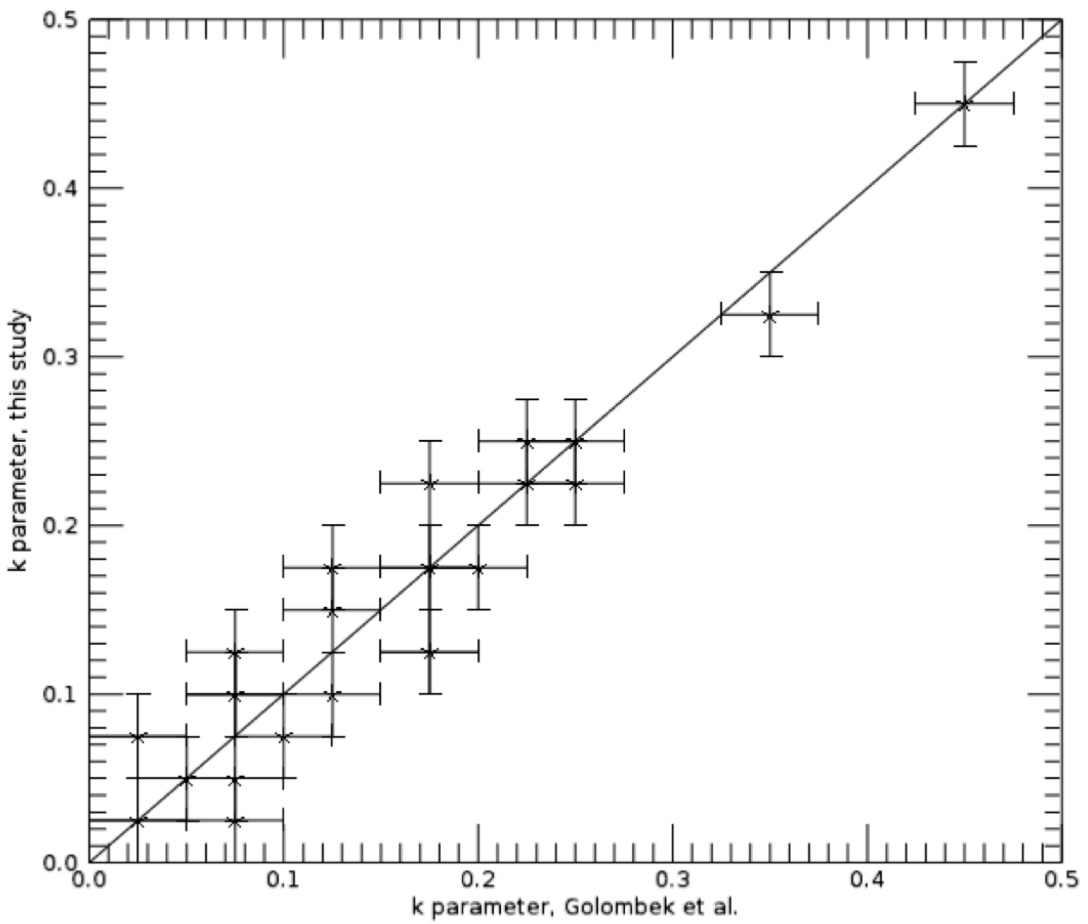

Figure 8. Comparison between cumulative fractional area covered by reliefs (k*) at different landing sites on Mars, measured in this study and in literature works. The values used in the comparison are taken from plots and maps in the literature and are shown here with an uncertainty of ±2.5 %.

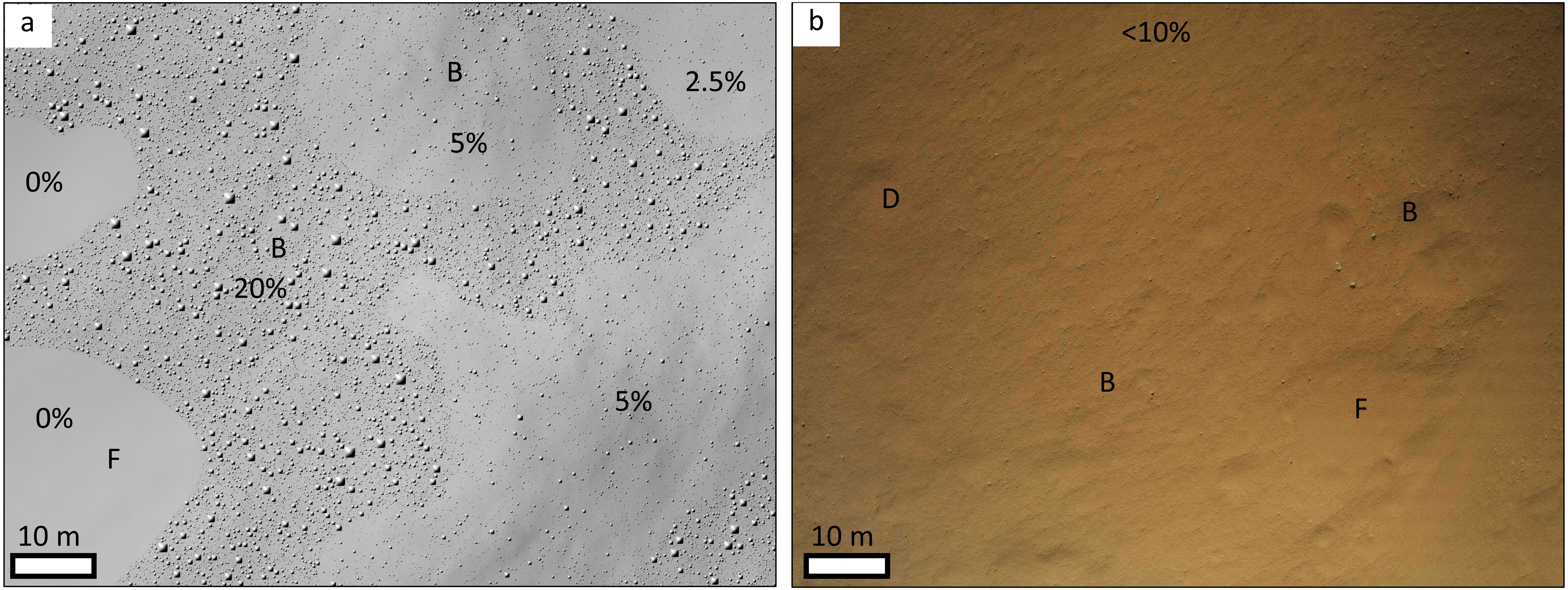

Figure 9. Qualitative comparison of the spatial pattern of roughness units between the synthetic topography at Oxia Planum shown as shaded relief (a,c) and a Mars Descent Imager (MARDI) image acquired during descent of the Curiosity rover at Gale crater (b,d). Common units are topographically flat and blocks-free ('F') and rough with varying amounts of blocks ('B'). Depressions are labeled 'D'. The synthetic image has units of different cumulative fractional area covered by blocks (CFA). The CFA at the Curiosity landing site has been estimated with HiRISE images to less than 10 % (Golombek et al., 2012). See main text for discussion.

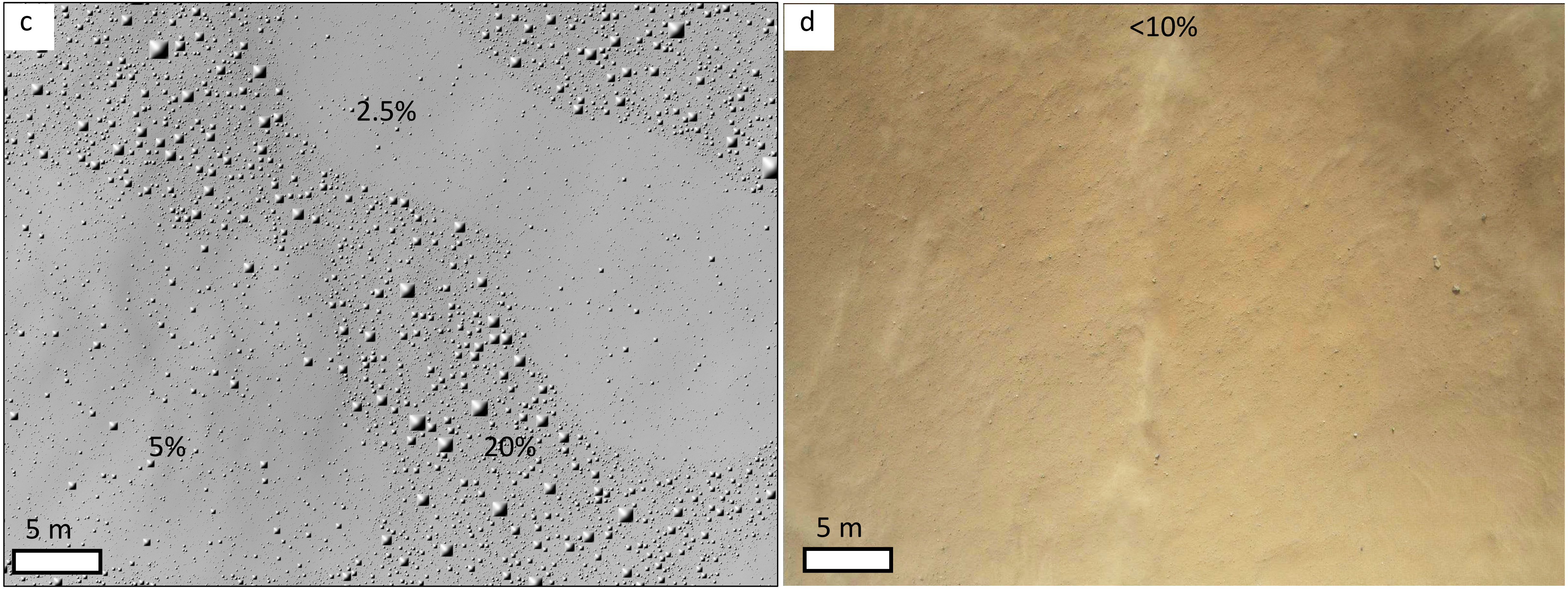

Figure 9. Qualitative comparison of the spatial pattern of roughness units between the synthetic topography at Oxia Planum shown as shaded relief (a,c) and a Mars Descent Imager (MARDI) image acquired during descent of the Curiosity rover at Gale crater (b,d). Common units are topographically flat and blocks-free ('F') and rough with varying amounts of blocks ('B'). Depressions are labeled 'D'. The synthetic image has units of different cumulative fractional area covered by blocks (CFA). The CFA at the Curiosity landing site has been estimated with HiRISE images to less than 10 % (Golombek et al., 2012). See main text for discussion.

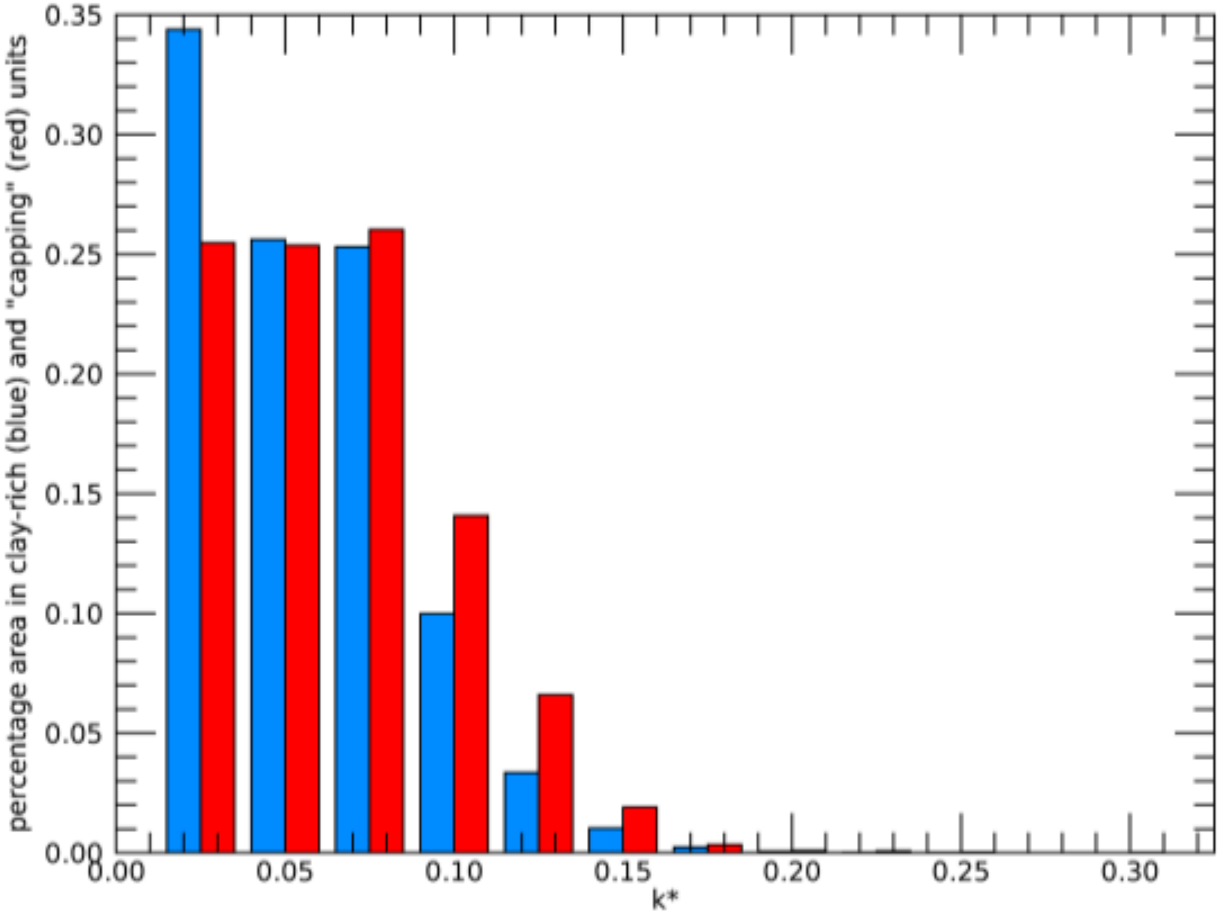

Figure 10. Distribution of the abundance of small-scale reliefs (k*) for the two major geological units at the Oxia Planum landing site: a clay-rich unit (blue) and a dark unit (red).

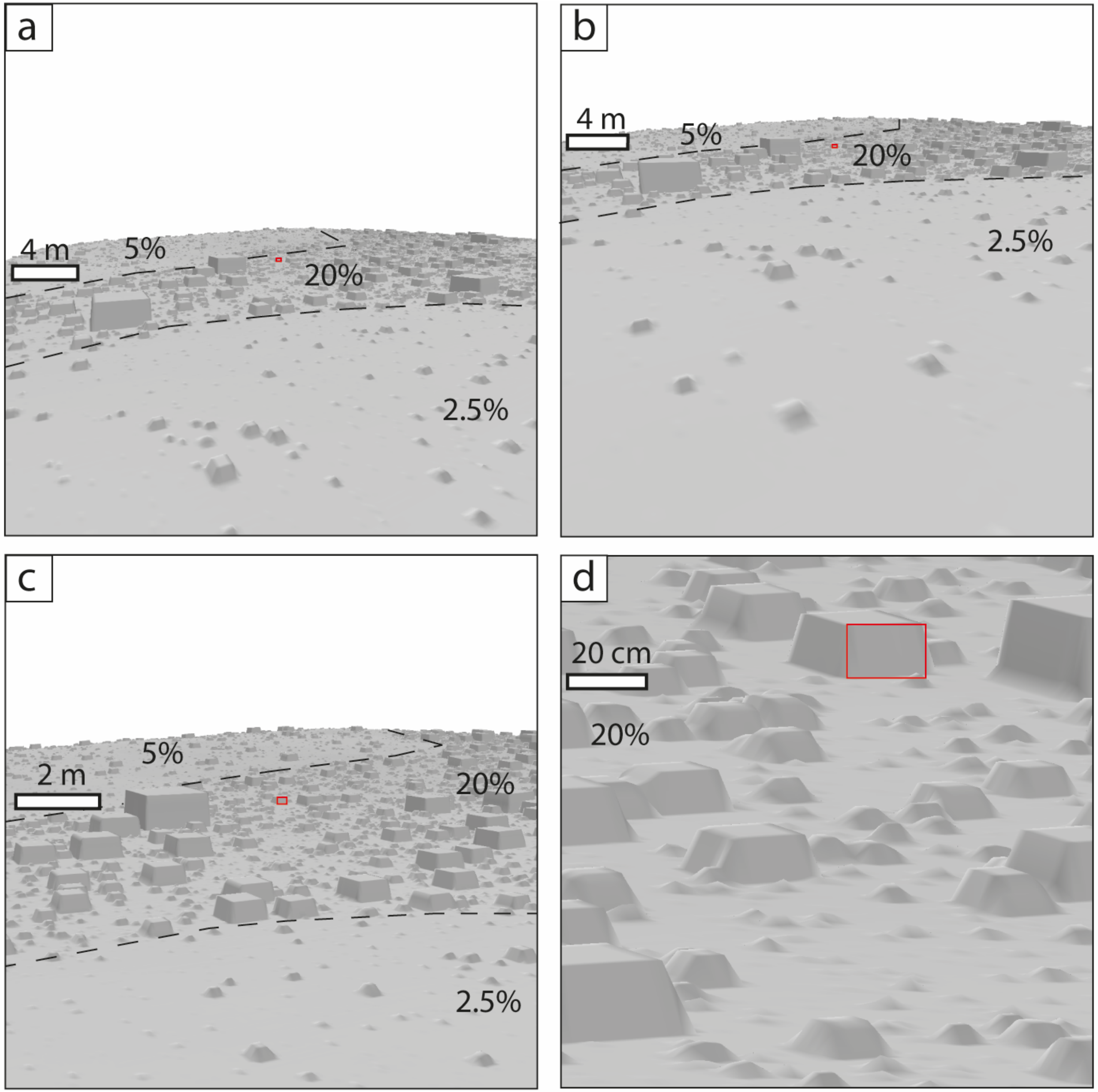

Figure 11. Modelled images by the ExoMars rover cameras. (a) NavCam, FOV 68°x68°. (b) LocCam, FOV 68°x68°. (c) One of two stereo images acquired by PanCam WAC, FOV 38°x38°. (d) PanCam HRC, FOV 4.8°x4.8°. All images are 1024x1024 pixels in size. Percentage values indicate fractional area covered by rocks. Dashed lines indicate boundary between different rock densities. The facet of a rock identifiable in all images is shown with a red box. The synthetic topography is illuminated with a light source at an angle of 60° above the horizon. Sky shown in white.

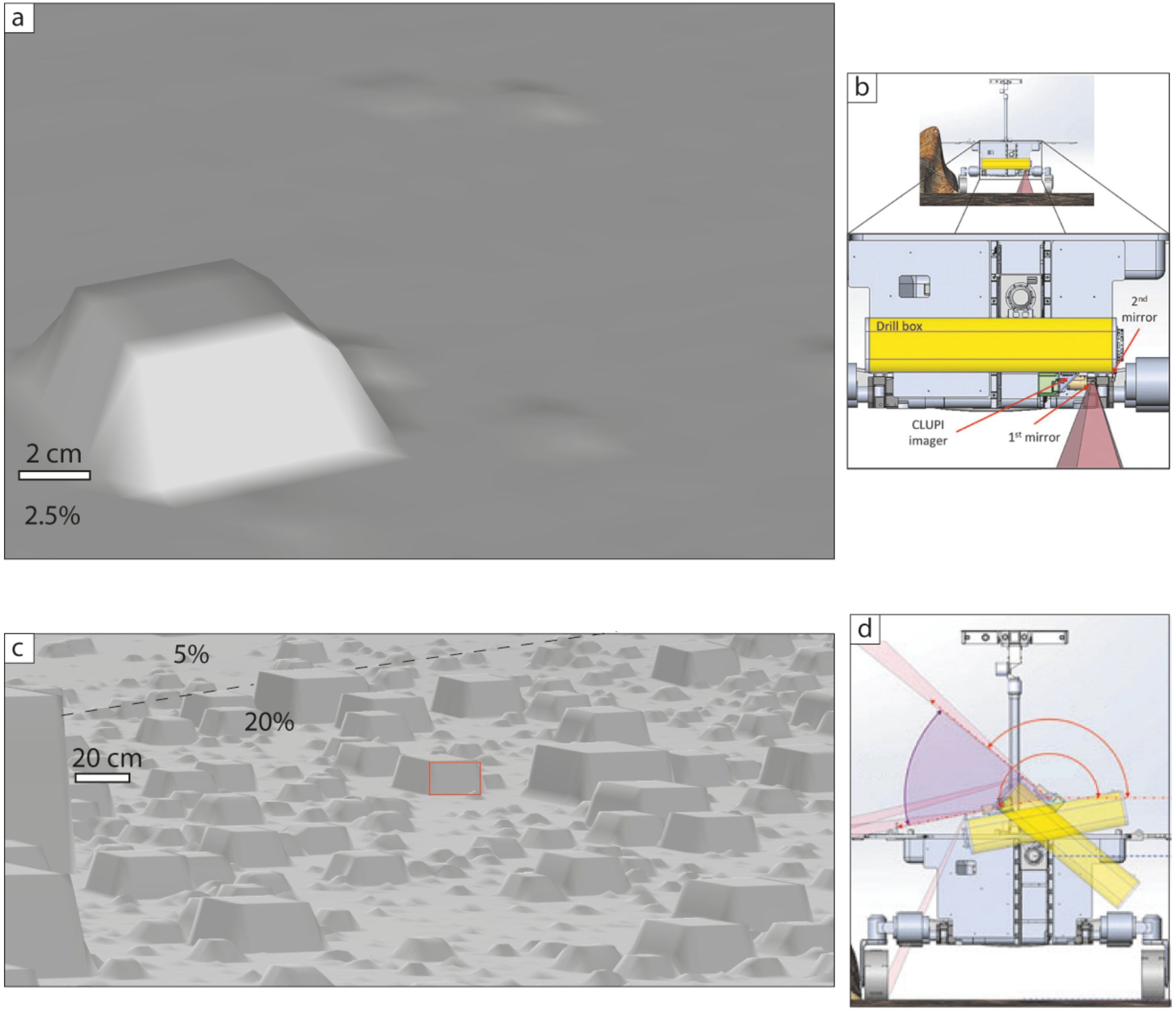

Figure 12. (a) CLUPI image in the geological environment survey mode with stowed drill and use of the primary mirror. The height of CLUPI is 40 cm. The entire FOV of 12°x8° is pointing 20° downwards from a horizontal plane and ahead of the rover. The synthetic topography is illuminated with a light source at an angle of <10° above the horizon to highlight cm-sized reliefs. Image 2652x1768 pixels in size. (b) Diagram of the position of CLUPI and the drill (yellow) corresponding to image acquisition in (a). (c) CLUPI image taken after the drill is lifted and rotated, and is pointing horizontally from a 1 m height. Image 2652x1128 pixels in size using the second mirror. The synthetic topography is illuminated with a light source at an angle of 60 ° above the horizon. (d) Diagram showing the lifted and rotated drill enabling CLUPI images at various elevations. Computer-aided design rendering (b) and (d) by Space Exploration Institute.

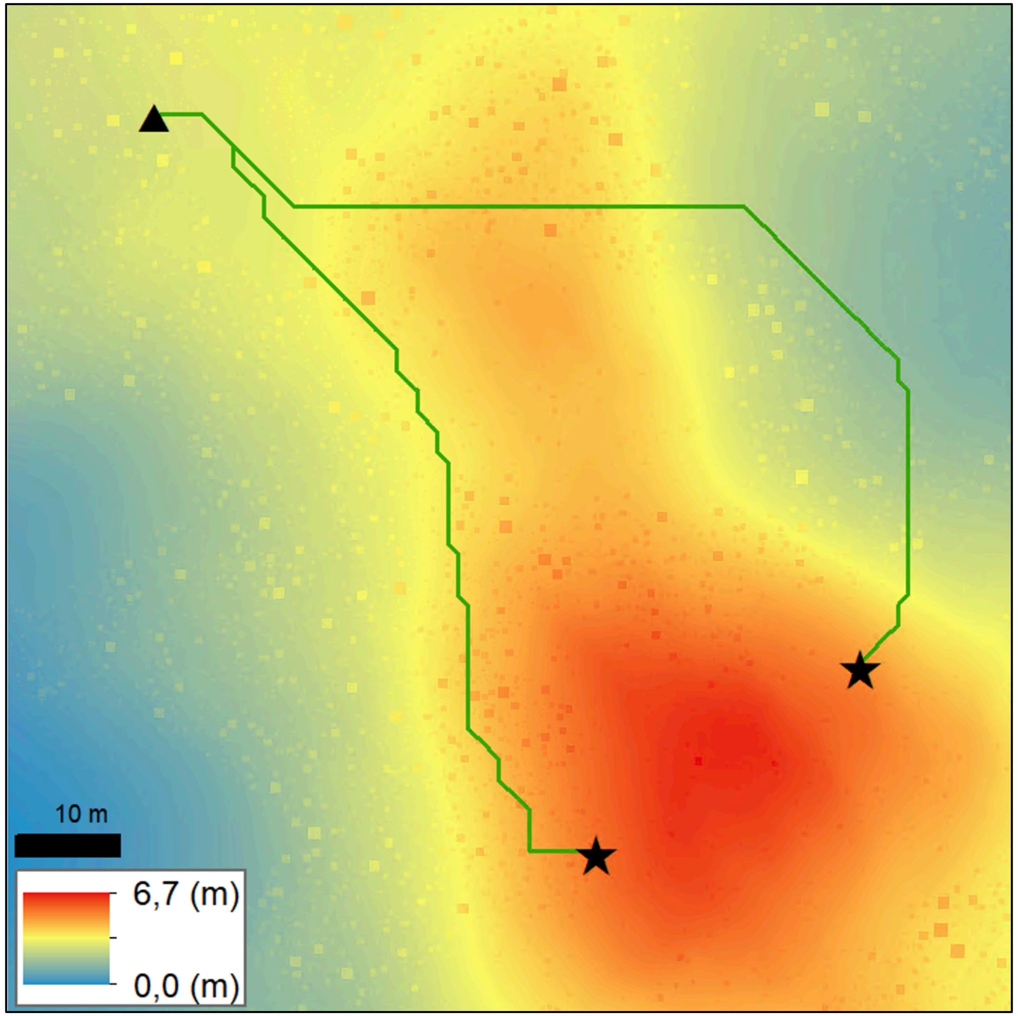

Figure 13. Rover traversability analysis on a color-coded synthetic topography. The triangle symbol is the start point and stars are target locations. Green lines are paths with the shortest traverse time calculated by considering the slope of the terrain and obstacles by small-scale reliefs.

Area	Lander observations	This study	Golombek et al. (2003)
Viking lander 1	8-10	10	8-10
Viking lander 2	15-20	15	30
Mars Pathfinder	12-20	7.5	10-20

Table 1. Cumulative fractional area covered by rocks (in %) at three landing sites. Estimates from ground truth observations and two HiRISE-based extrapolation methods.